Journal of Medicinal Chemistry

Article

pubs.acs.org/jmc

Reactive Oxygen Species (ROS) Inducible DNA Cross-Linking Agents and Their Effect on Cancer Cells and Normal Lymphocytes

Wenbing Chen,[†] Kumudha Balakrishnan,[‡] Yunyan Kuang,[†] Yanyan Han,[†] Min Fu,[‡] Varsha Gandhi,[‡] and Xiaohua Peng*[,†]

[†]Department of Chemistry and Biochemistry, University of Wisconsin—Milwaukee, 3210 N. Cramer Street, Milwaukee, Wisconsin 53211, United States

[‡]Department of Experimental Therapeutics, MD Anderson Cancer Center, Houston, Texas 77030, United States

Supporting Information

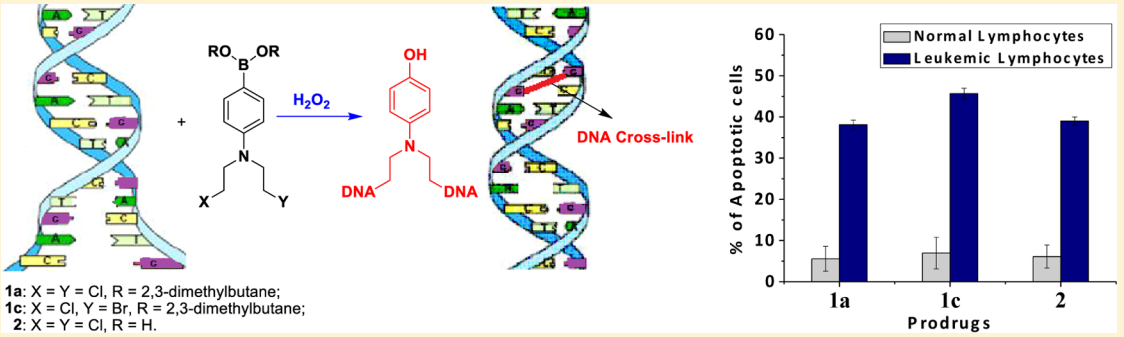

ABSTRACT: Reducing host toxicity is one of the main challenges of cancer chemotherapy. Many tumor cells contain high levels of ROS that make them distinctively different from normal cells. We report a series of ROS-activated aromatic nitrogen mustards that selectively kill chronic lymphocytic leukemia (CLL) over normal lymphocytes. These agents showed powerful DNA cross-linking abilities when coupled with H_2O_2, one of the most common ROS in cancer cells, whereas little DNA cross-linking was detected without H_2O_2. Consistent with chemistry observation, in vitro cytotoxicity assay demonstrated that these agents induced 40−80% apoptosis in primary leukemic lymphocytes isolated from CLL patients but less than 25% cell death to normal lymphocytes from healthy donors. The IC_{50} for the most potent compound (**2**) was ~5 μM in CLL cells, while the IC_{50} was not achieved in normal lymphocytes. Collectively, these data provide utility and selectivity of these agents that will inspire further and effective applications.

INTRODUCTION

Making use of the unique property of cancer cells is one of the most important avenues to design targeted anticancer drugs. Many types of cancer cells are under oxidative stress because of their disturbed intracellular redox balance, which makes them distinct from their "healthy" counterparts.[1−5] The increased amounts of reactive oxygen species (ROS) can be a therapeutic advantage because it is an intrinsic feature of cancer cells.[6−9] Recently, several anticancer agents based on the ROS-mediated mechanisms have been developed to target these specific tumor cells and have shown selective killing of cancer cells.[10−14] For example, Huang and co-workers reported that β-phenethyl isothiocyanate[10] and 2-methoxyoestradiol[11] selectively killed human leukemia cells but not normal lymphocytes by causing further ROS stress in cancer cells. Piperlongumine was also found to selectively kill cancer cells by increasing ROS levels but had little effect on primary normal cells.[13,14] Most of the existing ROS-targeting drugs focus on enhancing ROS production to inflict lethal damage. To the best of our knowledge, the drug design for targeting tumor cells containing high levels of ROS via inducing DNA interstrand cross-links (ICLs) is rarely reported.

DNA ICLs are recognized as the primary mechanism for the cytotoxic activity of many clinically useful antitumor drugs, such as chlorambucil, cyclophosphamide, bendamustine, and cisplatin. However, the severe host toxicity exhibited by these anticancer drugs continues to be a major problem in cancer chemotherapy. Prodrugs that are activated specifically in tumor cells have the potential to reduce the toxicity of the cross-linking agents for normal cells. Gates and co-workers demonstrated that several anticancer drugs displayed selective toxicity by releasing DNA damaging species selectively in tumor cells.[15−17] Over the past few decades, several research groups have developed novel DNA cross-linking or alkylating agents that can induce ICL formation by oxidation, reduction, or photolysis.[18−25] Recently, our group has shown that H_2O_2-induced DNA cross-linking behaviors provided a novel strategy for tumor-specific damage.[26,27] H_2O_2 is one of the most

Received: September 2, 2013
Published: May 6, 2014

common ROS, which is believed to be produced in large amounts in several human tumor cells.[1−5] The transformed cells showed more than 10-fold increase in H_2O_2 levels.[28a] Different from $O_2^{\bullet-}$ or hydroxyl radicals that are extremely unstable, H_2O_2 has the chemical stability required to establish significant steady-state concentrations in vivo and is uncharged. These properties allow H_2O_2 to freely diffuse across plasma membranes and to travel to the cells. In addition, other ROS such as O_2 can also be reduced to H_2O_2 in the oxygen metabolism via $O_2^{\bullet-}$ generation involved in hypoxia-inducible factor 1 (HIF-1) regulation.[28b,c] Thus, developing H_2O_2-activated prodrugs to selectively kill ROS-containing cancer cells can be a potent strategy in cancer chemotherapies.

Such agents should consist of two separate functional domains: an efficient H_2O_2-responsive moiety "trigger" and a potent cell-damaging functional group "effector", joined by a linker system in such a way that the reaction of the trigger with H_2O_2 causes a large increase in the cytotoxic potency of the effector (Scheme 1). The selective reaction of boronic acid or ester derivatives with H_2O_2 has been applied for fluorescent detection of H_2O_2, gene expression, point-of-care assay, and prodrug development.[26,27,29−37] Recently, we have developed two types of H_2O_2-activated DNA cross-linking agents using boronic acid or ester as "trigger". One class can release a nitrogen mustard effector upon treatment with H_2O_2, while the other can produce quinone methides cross-linking DNA. However, both did not show potent anticancer activity. We speculate that these charged molecules may not be suitable for drug development because it is well-known that charged molecules cannot diffuse across cell membrane. Here, we report a novel strategy for creating neutral H_2O_2-activated prodrugs that showed dramatically increased potency and selective cytotoxicity toward various cancer cells. For the first time we demonstrated that the direct attachment of a boron group to an aromatic ring is sufficient to mask the toxicity of the nitrogen mustard. The potential therapeutic utility has been demonstrated by determining their toxicity and selectivity toward primary leukemic lymphocytes from CLL patients and comparing that with normal lymphocytes from healthy donors.

We designed and synthesized a series of H_2O_2-activated boron-containing aromatic nitrogen mustard prodrugs (**1**−**3**) with two linker systems and various leaving groups. Compounds **1a**−**f** and **2** contain a nitrogen mustard group directly bonded to the aromatic ring (Scheme 2A). The electron-withdrawing boronate group decreases the electron density of the benzene ring and makes the lone pair of the nitrogen mustard delocalize to boron (**D**). Therefore, these prodrugs do not form the electrophilic aziridinium ring **E** and are not deleterious to cells with low ROS levels (Scheme 2B). However, the oxidation of the carbon−boron bond by H_2O_2 followed by a transformation to a hydroxyl group can trigger an increased electron release to the nitrogen of the mustard moiety (**B**);[29] this facilitates the formation of a highly electrophilic aziridinium ring **C** capable of cross-linking DNA. Compound **3** contains a withdrawing carbonyl group that can reduce the toxicity of the nitrogen mustard. We assumed that release of the amine effector would occur upon activation of **3** by H_2O_2.[30−32]

Scheme 1. Selective DNA Cross-Linking Agent with a ROS-Responsive "Trigger" and an "Effector"[a]

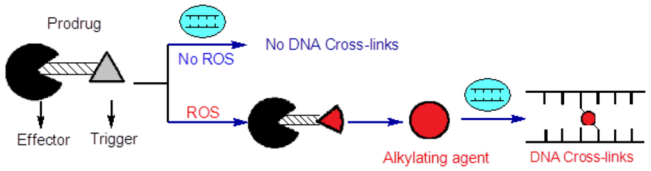

[a]DNA ICL was not formed in the absence of ROS, as the "effector" was deactivated in the prodrug, while in a ROS-containing environment, the reaction of the trigger unit with ROS activated the "trigger−effector" system resulting in a potent DNA cross-linking agent ("trigger" changes from a gray triangle to a red sector leading to a complete red circle).

Scheme 2. (A) Structures of the Designed Prodrugs and (B) Mechanism of Targeting ROS-Containing Cancer Cells

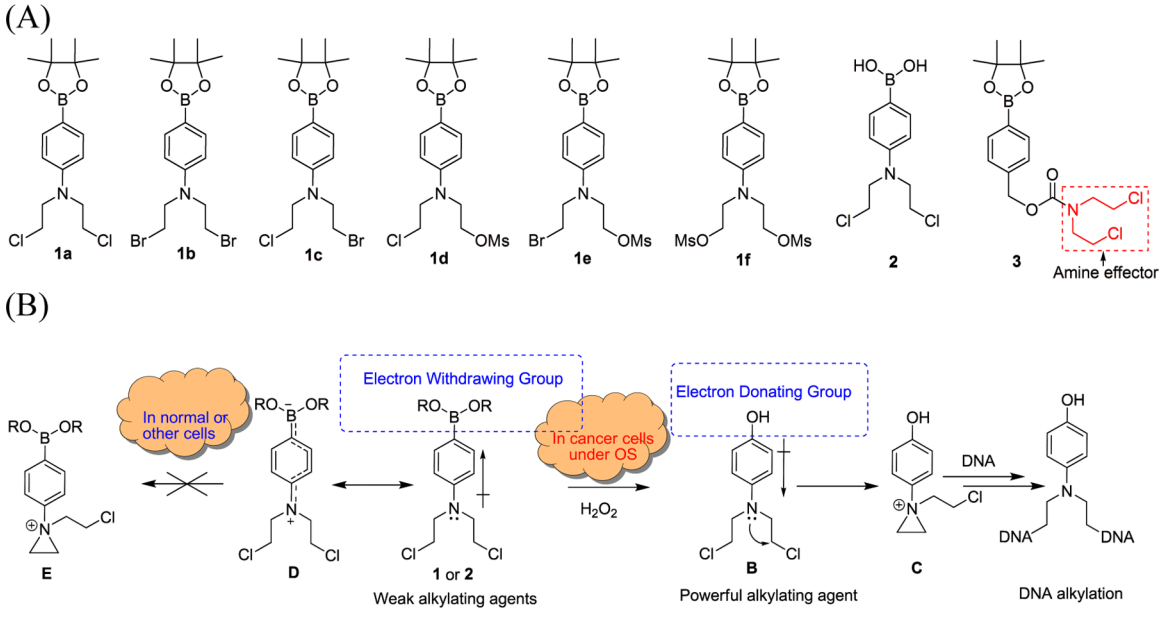

dx.doi.org/10.1021/jm401349g | J. Med. Chem. 2014, 57, 4498−4510

Scheme 3. Synthesis of Compounds 1a–f (A), 2 (B), and 3 (C)

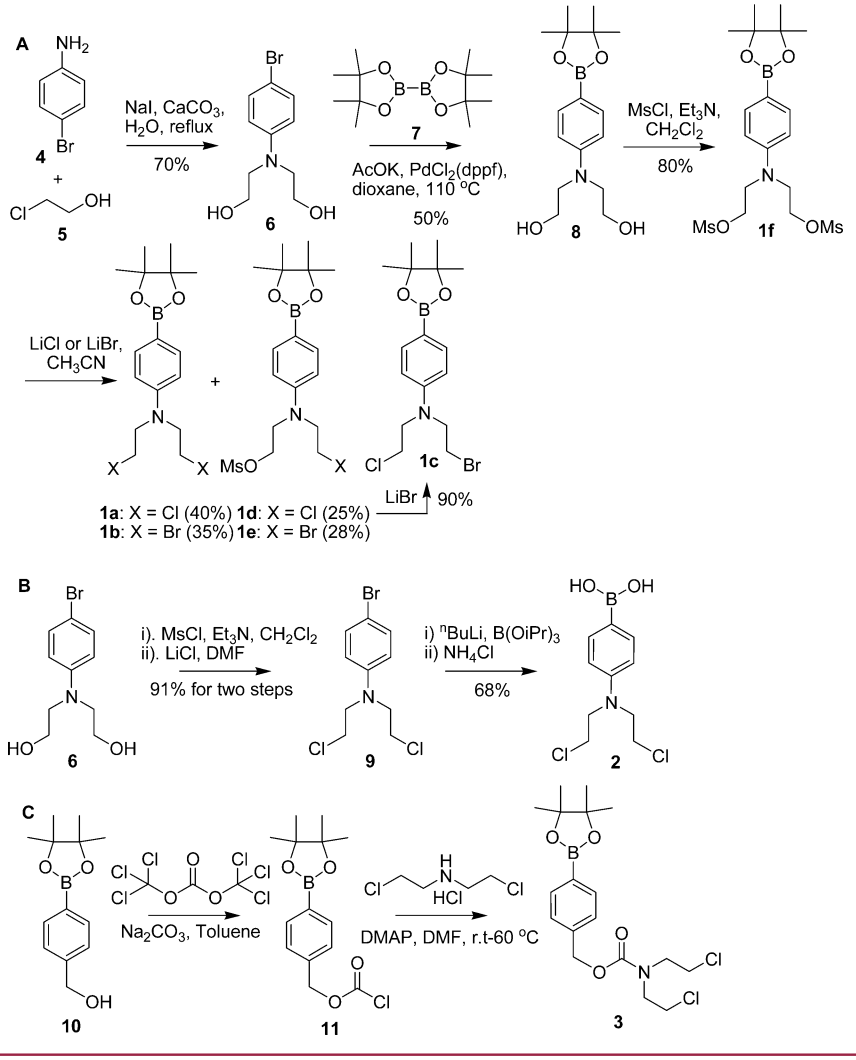

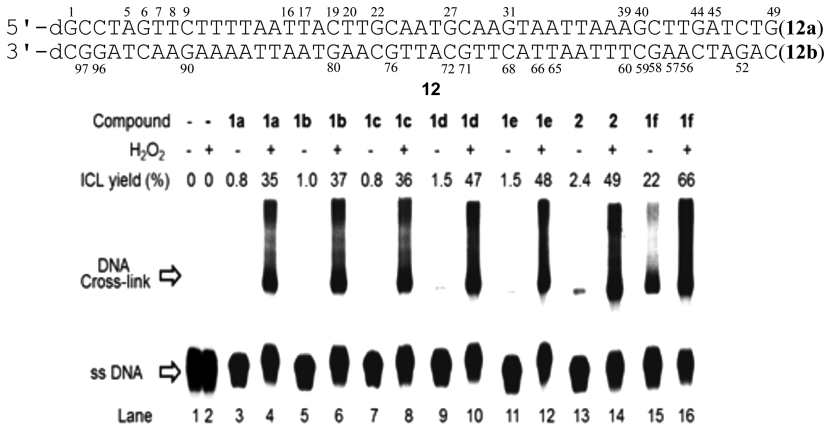

Figure 1. Comparison of the H_2O_2-inducible activity and selectivity of **1a–f** and **2**. Phosphorimage autoradiogram of denaturing PAGE analysis of the cross-linking reaction of DNA duplex **12** in the presence of **1a–f** or **2** (1.0 mM) (all reactions were carried out at room temperature).

RESULTS

Synthesis of 1a–f, 2, and 3. The synthesis of compounds **1–3** is shown in Scheme 3. Compounds **1a–f** and **2** were synthesized starting from *p*-bromoaniline (**4**). 2-Chloroethanol was first coupled with **4** using calcium carbonate as a base yielding **6**. Palladium-catalyzed borylation of **6** provided boronate intermediate **8** which reacted with MsCl resulting in dimesylate mustard **1f** at 80% yield. Nucleophilic substitution of **1f** with 1.0 equiv of lithium chloride or lithium bromide afforded **1a**, **1d** or **1b**, **1e** respectively. Compound **1d** was converted to **1c** by further treatment with lithium bromide (Scheme 3A). For the synthesis of boronic acid **2**, compound **6** was first converted to dichloromustard **9** via mesylation and chlorination (Scheme 3B), and treatment of **9** with butyllithium

dx.doi.org/10.1021/jm401349g | J. Med. Chem. 2014, 57, 4498–4510

and triisopropyl borate was followed by hydrolysis that yielded boronic acid **2**. Compound **3** was obtained via an amidation reaction of bis(2-chloroethyl)amine hydrochloride and chloroformate **11** which was synthesized from **10** and triphosgene (Scheme 3C).

Selective DNA Cross-Linking Ability. Initially we investigated their DNA cross-linking abilities and selectivity by allowing cross-linkers to react with DNA duplex **12** which contains GNC sequences at the terminus. First, we studied the effect of the carbamate linker (**3**) on the activity of nitrogen mustard. As we expected, **3** did not induce ICL formation in the absence of H_2O_2, which indicated that a carbamate linker is sufficient to deactivate the nitrogen mustard. To our surprise, DNA ICLs were not formed in the presence of **3** and H_2O_2. Obviously, a carbamate linker is not suitable for constructing H_2O_2-inducible DNA cross-linking agents.

Next, we studied the reactivity of **1a**–**f** and **2** toward **12** (Figure 1). In the absence of H_2O_2, no obvious DNA ICLs were observed for **1a**–**e** and **2**, while **1f** induced 22% DNA cross-linking. Compound **1f** contains two mesylate groups, while the others have one (**1d** and **1e**) or no mesylate group (**1a**-**1c** and **2**). The better leaving property of the mesylate group may cause the higher reactivity of **1f** compared to others in a H_2O_2-free system. These data indicated that boron groups are sufficient to deactivate dihalogen or halogenmesylate mustards but cannot completely mask the reactivity of dimesylate mustard **1f**. The addition of H_2O_2 triggered the activity of **1a**–**e** and **2**, leading to efficient ICL formation (37%–49%). Similarly, the cross-linking yield of **1f** was increased 3-fold upon H_2O_2 activation. It is worth mentioning that the ICL was not observed when the DNAs were treated with H_2O_2 only (Figure 1, lane 2). As we proposed, the conversion of an electron-withdrawing boron group to a donating hydroxyl group by H_2O_2 increases the electron density of nitrogen mustard and therefore facilitates the ICL formation (Scheme 2B). DNA ICLs induced by **1a**–**f** and **2** were observed at a concentration as low as 50 μM (~3% ICL yield), and the optimum ratio of drug to H_2O_2 was 1:2 (Tables S1–S7 and Figures S2–S3). The best selectivity and activity were observed under physiological pH and temperature (pH 7.0–8.0 and 37.0–38.0 °C) (Figure S4 and S5). The ICL production induced by these compounds followed first-order kinetics with a rate constant (k_{ICL}) ranging from $(2.45 \pm 0.25) \times 10^{-5}$ s^{-1} to $(5.42 \pm 0.15) \times 10^{-5}$ s^{-1} (Figure S6). Among these agents with different leaving groups, compounds with the methyl mesylate group showed a higher H_2O_2-inducible DNA cross-linking ability than those having halogen groups with an order of **1f** > **1d** ~ **1e** >**1a** ~ **1b** ~ **1c**. Upon treatment of H_2O_2, **1f** with two mesylate groups resulted in 66% DNA ICLs, while **1d** and **1e** with one mesylate group and one halogen group produced 47% and 48% ICL, respectively. Lastly only 35%–37% yields were observed with **1a**, **1b**, and **1c** with two halogen groups. Besides that, no obvious different reactivity was found in compounds with bromine or chlorine groups (**1d** vs **1e**; **1a** vs **1b** vs **1c**).

In order to understand whether the location of GNC sequences affects the cross-linking efficiency, we synthesized duplex **12′** with GNCs in the middle of the sequence and investigated ICL formation of duplex **12′** induced by **1a**/H_2O_2 and **1b**/H_2O_2 (1 mM). The cross-linking yield of **12′** (27% ± 3.5) was slightly lower than that of duplex **12** (35% ± 4.0), but both are within the experimental error of each other (Figure S7). These data showed that the activity and selectivity of these agents can be achieved with a variety of DNA sequences. It is necessary to point out that smearing bands were observed when the cross-linking yield was high and/or when there were multiple cross-linking sites or alkylating sites, while such phenomena were not observed when the yields were low (Figures S6F and S8).

Subsequently, we investigated the activity of **1a**, **1d**, and **2** toward other ROS including *tert*-butyl hydroperoxide (TBHP), OCl^-, HO·, ^tBuO·, O_2^-, and NO (Figure S8). Among these, H_2O_2 is the most efficient ROS that triggers the activity of these prodrugs, while TBHP, OCl^-, and O_2^- also slightly activate **1a**, **1d**, and **2**. In the presence of H_2O_2, these compounds induced 30–47% ICL formation, while much lower ICL yields were observed with other ROS (0.9–6.6% for OCl^-, 1.0–3.6% for TBHP, and 5–15% for O_2^-) (Figure 2). This is consistent with previous reports about the selective reaction of boronic acids and their esters toward H_2O_2.[26,30]

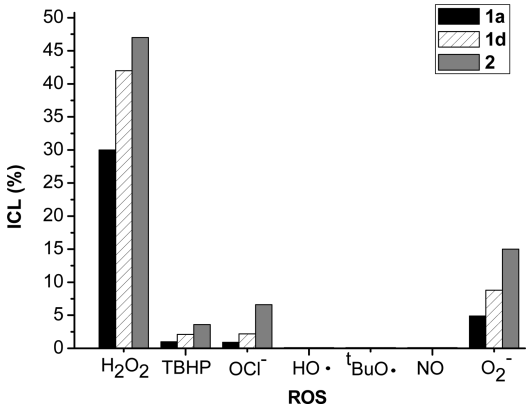

Figure 2. ICL formation induced by **1a**, **1d**, and **2** upon treatment with various ROS (1 mM of drugs and ROS were used).

NMR Detection of Activation of 1a and 2 by H_2O_2. Activation of **1a** and **2** by H_2O_2 and the formation of hydroxyl analogue **13** were confirmed by NMR analysis (Figures 3–5). The reaction of **1a** (20 μmol) or **2** (20 μmol) with H_2O_2 (30 μmol) was carried out in a mixture of 400 mM deuterated potassium phosphate buffer (pH 8.0) (50 μL) and DMSO-d_6 (450 μL). In the presence of H_2O_2, oxidative deboronation of

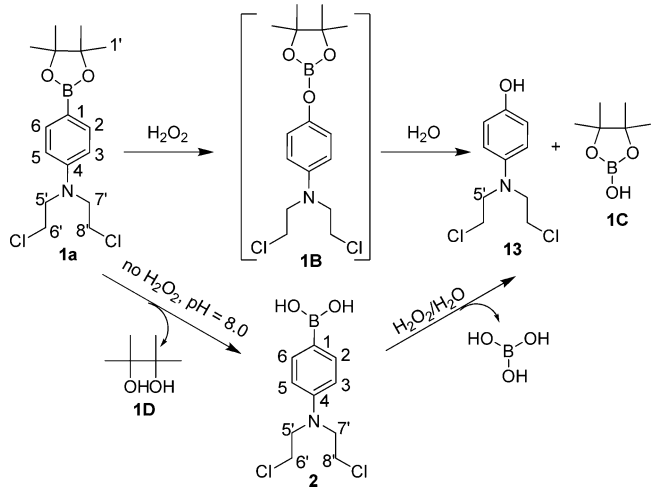

Figure 3. Activation of **1a** and **2** by H_2O_2.

dx.doi.org/10.1021/jm401349g | J. Med. Chem. 2014, 57, 4498–4510

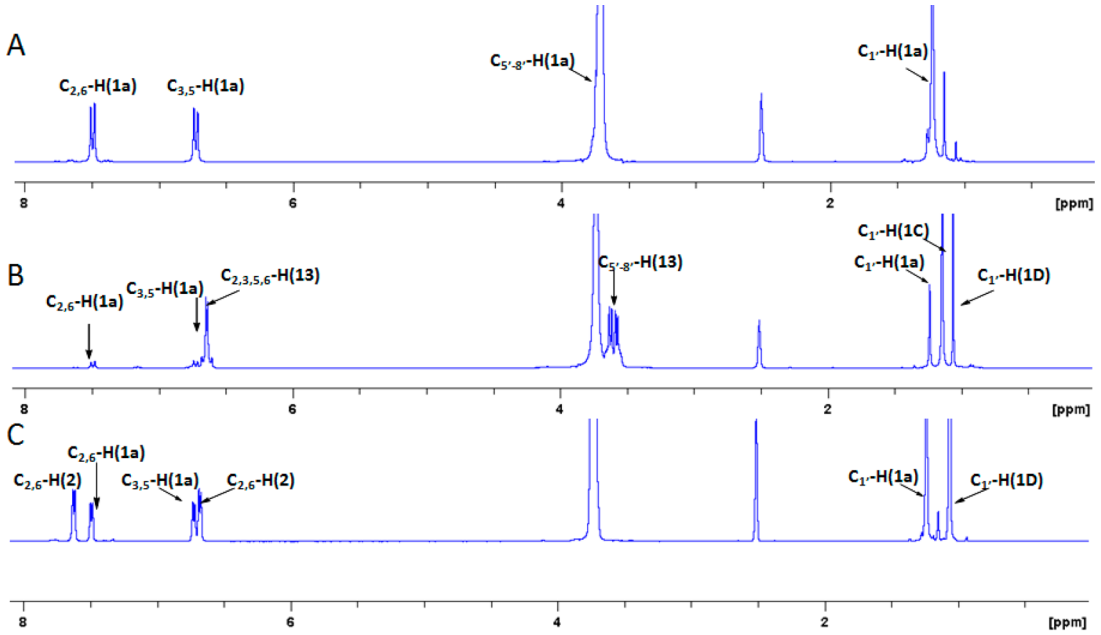

Figure 4. ^{1}H NMR analysis of the activation of **1a** (40 mM) by H_2O_2 (60 mM): (A) ^{1}H NMR analysis of **1a** in 400 mM phosphate buffer (pH 8) (50 μL)/DMSO-d_6 (450 μL); (B) 30 min after the addition of H_2O_2; (C) 24 h after **1a** was incubated in 4.0 mM deuterated potassium phosphate buffer in the absence of H_2O_2 (1.0 M deuterated potassium phosphate buffer/DMSO-d_6/D_2O = 2:450:48).

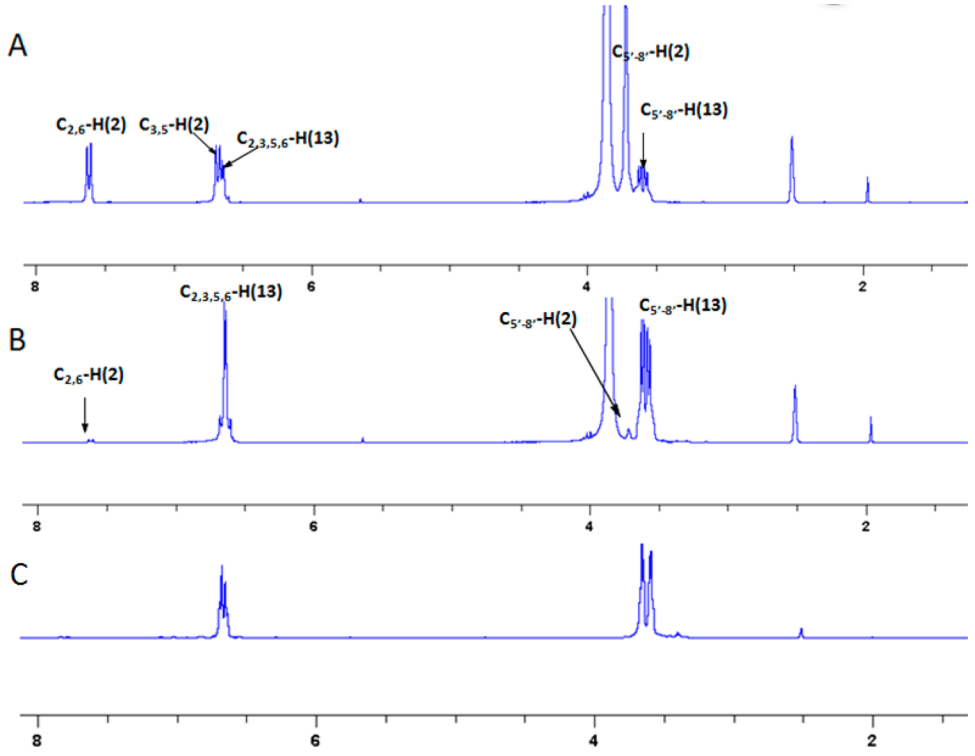

Figure 5. ^{1}H NMR analysis of the activation of **2** (40 mM) by H_2O_2 (60 mM): (A) 5 min after the addition of H_2O_2; (B) 2 h after the addition of H_2O_2 [the reaction was carried out in 1.0 M deuterated phosphate buffer (pH 8) (100 μL)/DMSO-d_6 (450 μL)]; (C) an authentic sample of compound **13** in D_2O (100 μL)/DMSO-d_6 (450 μL).

1a occurred yielding alkylating agent **13** and boronic acid (**1C**), which was evidenced by the appearance of $C_{1'}$-H (δ 1.26 for **1a** and δ 1.14 for **1C**) (Figure 4). Compound **1C** was further hydrolyzed to pinacol (**1D**, δ 1.06). The intermediate **1B** was too active to be detected. The conversion of **1a** to **13** was so fast that more than 80% of **1a** to **13** was completed within 30 min, and >95% of **13** was formed after 2 h, which showed that the aryl boronates developed in this work are efficient H_2O_2-responsive trigger units. To ensure the role of H_2O_2 in activation, a control experiment was performed by incubating **1a** in potassium phosphate buffer in the absence of H_2O_2 (Figure 4C). The activated product **13** was not detected, while hydrolysis of **1a** occurred leading to **2** and pinacol. Compound **2** can also be efficiently converted to **13** by H_2O_2; 93% of **2** was

dx.doi.org/10.1021/jm401349g | J. Med. Chem. 2014, 57, 4498−4510

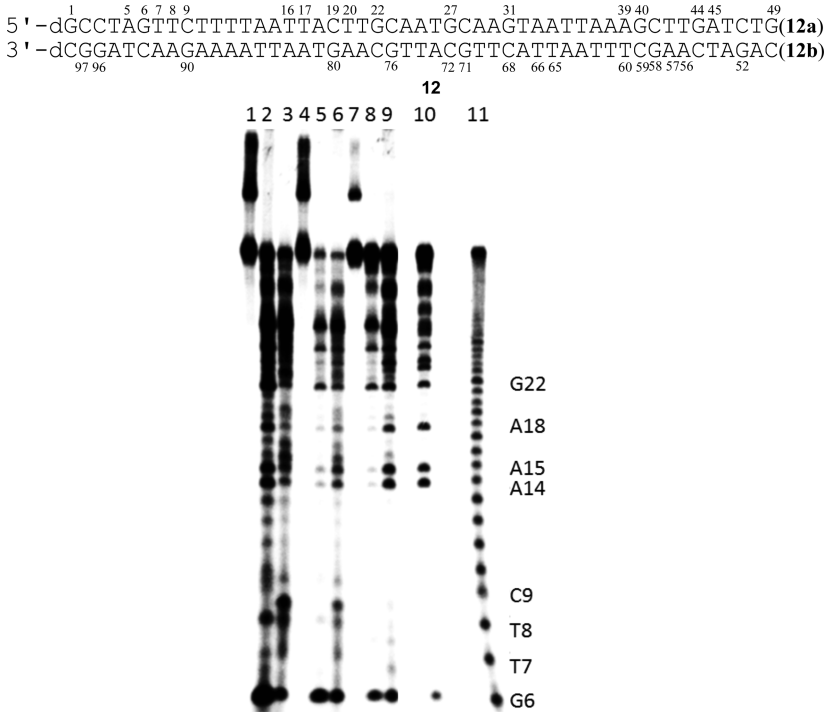

Figure 6. Comparison of specific cross-linking sites caused by **1a**/H_2O_2, **13**, and mechlorethamine. Phosphorimage autoradiogram of 20% denaturing PAGE analysis of the ICL products upon heating in piperidineor phosphate buffer. The ICL products were produced by incubation of duplex **12** with **1a**/H_2O_2, **13**, or mechlorethamine. **12a** was radiolabeled at 5′-terminus. Lanes 1−3, **1a**/H_2O_2; lanes 4−6, compound **13**; lanes 7−9, mechlorethamine; lanes 1, 4, 7, control (no treatment); lanes 2, 5, 8, treated by heating at 90 °C in buffer (pH 7.0); lanes 3, 6, 9, treated by heating at 90 °C in piperidine; lane 10, G + A sequencing; lane 11, Fe·EDTA treatment of **12**.

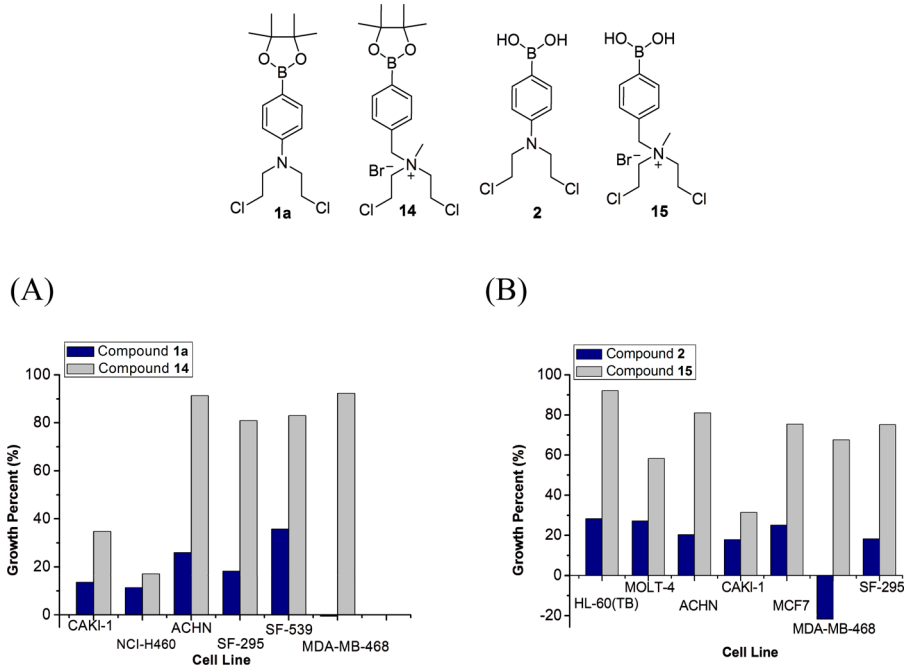

Figure 7. Comparison of the anticancer activities of prodrugs with the ones releasing mechlorethamine. Each cell line was grown in two plates and treated with drug (10 μM) for 48 h at 37 °C, 5% CO_2, 95% air, and 100% relative humidity. The growth percents were determined by NCI-60 DTP human tumor cell line screen:[40] (A) **1a** vs**14**; (B) **2** vs **15**.

converted to **13** within 2 h (Figure 5). Overall, the prodrugs developed in this work are sensitive to H_2O_2 under physiological conditions.

In order to confirm that **13** was the direct alkylating agent generated from **1a** or **2** with H_2O_2, we isolated **13** from the reaction of **2** with H_2O_2 in potassium phosphate buffer (Figure S1). The reaction was so efficient that 85% (isolated yield) of **13** was obtained after 2 h. Compound **13** was characterized by ^{1}H NMR, ^{13}C NMR, and high resolution mass spectrometry (Supporting Information). Its reactivity with DNA was also

dx.doi.org/10.1021/jm401349g | J. Med. Chem. 2014, 57, 4498−4510

Table 1. Cytotoxicities of 1a, 1c, 1d, and 2

		GI_{50} (μM)			
tumor type	cell line	**1a**	**1c**	**1d**	**2**
leukemia	CCRF-CEM	3.34	5.03	4.01	3.27
	HL-60(TB)	4.66	5.11	3.88	2.88
	K-562	17.2	22.6	19.0	15.8
	MOLT-4	3.48	3.69	3.74	2.90
	RPMI-8226	10.90	19.40	14.7	8.59
	SR	**0.63**	**0.66**	**0.63**	**0.48**
non-small-cell lung	A549/ATCC	2.69	4.88	4.98	0.89
	EKVX	18.6	22.5	24.5	15.4
	HOP-62	10.9	10.9	8.85	8.48
	HOP-92	9.24	12.80	11.5	10.50
	NCI-H226	12.9	11.9	10.4	10.3
	NCI-H23	4.57	5.38	4.70	3.36
	NCI-H322M	14.7	32.5	28.2	15.1
	NCI-H460	**0.33**	**0.42**	**0.49**	**0.23**
	NCI-H522	6.59	11.70	5.99	3.53
colon cancer	COLO 205	11.60	11.40	11.00	7.26
	HCC-2998	14.9	24.0	14.6	12.1
	HCT-116	11.60	13.90	11.10	9.37
	HCT-15	13.20	17.10	13.50	9.46
	HT29	13.8	18.8	14.6	11.9
	KM12	14.9	31.3	25.8	15.1
	SW-620	11.30	13.90	11.90	8.39
CNS	SF-268	4.61	4.90	5.39	4.72
	SF-295	2.11	2.64	2.99	1.36
	SF-539	5.70	6.37	4.83	3.35
	SNB-19	8.06	10.60	10.20	8.00
	SNB-75	7.98	10.70	5.85	3.21
	U251	**3.75**	**5.07**	**0.70**	**3.49**
melanoma	LOX IMVI	5.17	6.60	4.72	3.13
	MALME-3M	17.5	18.4	14.0	19.7
	M14	5.10	7.86	5.68	4.77
	MDA-MB-435	14.2	16.5	15.3	13.0
	SK-MEL-2	22.1	20.8	21.5	19.0
	SK-MEL-28	21.0	20.6	15.6	13.5
	SK-MEL-5	14.5	13.7	12.8	10.9
	UACC-257	11.6	13.4	13.0	11.6
	UACC-62	6.12	9.38	5.83	4.71
ovarian	IGROV1	15.6	19.1	13.6	18.1
	OVCAR-3	14.6	15.0	13.4	12.0
	OVCAR-4	17.4	14.4	13.9	12.1
	OVCAR-5	21.6	25.9	22.9	16.0
	OVCAR-8	7.83	11.90	8.20	4.20
	NCI/ADR-RES	5.33	6.69	6.52	2.69
	SK-OV-3	8.03	9.25	8.96	3.81
renal	786-0	5.35	8.95	6.55	4.04
	A498	2.81	5.87	8.59	3.43
	ACHN	3.64	3.40	3.03	1.75
	CAKI-1	2.78	3.52	3.10	1.44
	RXF 393	10.3	10.4	5.71	2.55
	SN12C	4.11	4.45	4.40	2.08
	TK-10	16.7	22.6	18.0	15.5
	UO-31	5.78	6.51	6.18	6.05
prostate	PC-3	14.30	17.70	15.10	15.10
	DU-145	4.25	6.69	4.52	4.89
breast	MCF7	4.12	5.03	4.44	1.89
	MDA-MB-231/ATCC	16.5	22.8	22.1	16.6
	HS 578T	26.2	27.4	24.1	31.4
	BT-549	10.5	12.1	12.0	6.63
	T-47D	10.70	12.00	8.49	6.29

dx.doi.org/10.1021/jm401349g | J. Med. Chem. 2014, 57, 4498−4510

Table 1. continued

tumor type	cell line	GI_{50} (μM) 1a	1c	1d	2
	MDA-MB-468	**1.60**	**1.49**	**1.07**	**0.51**

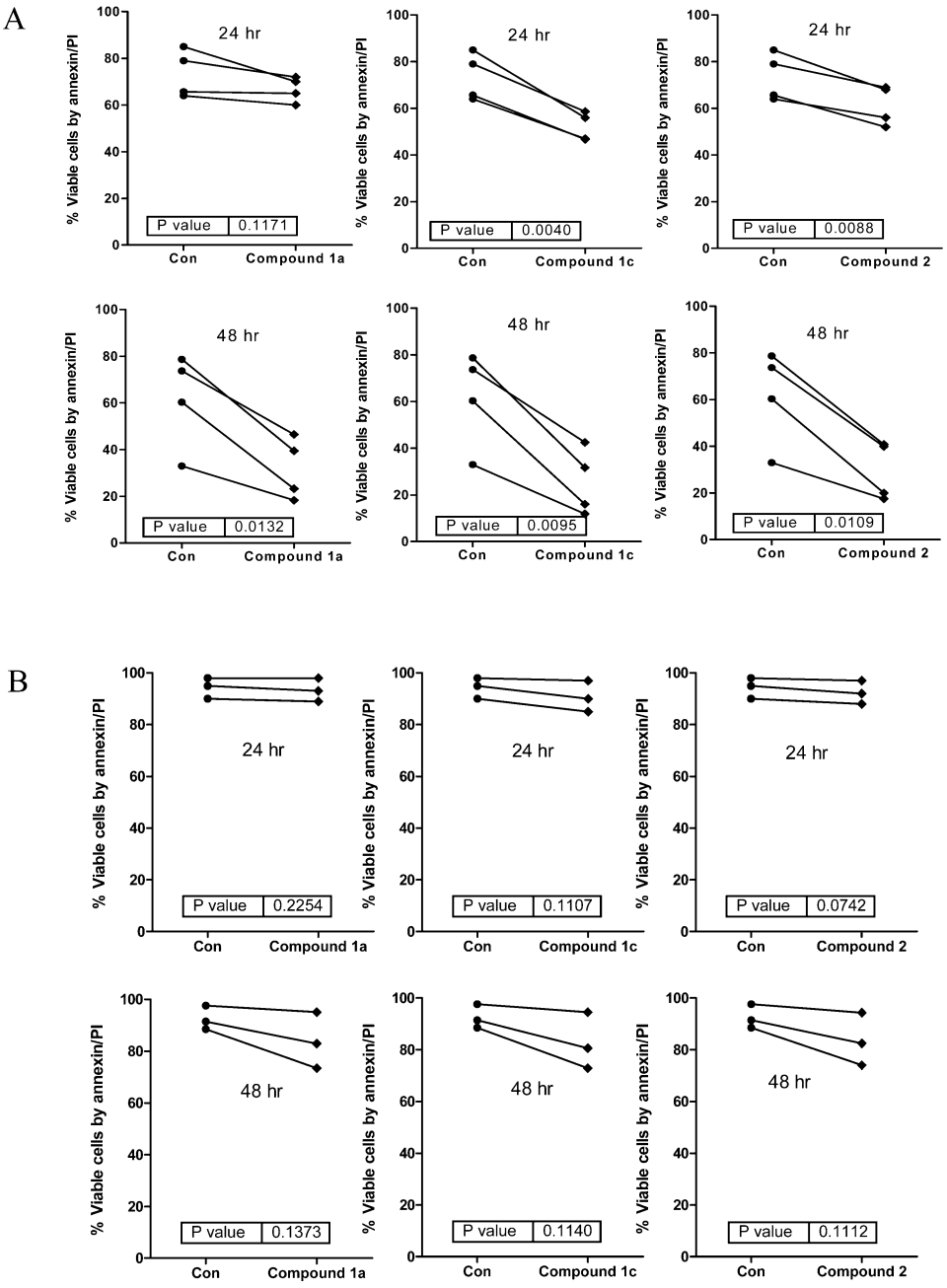

Figure 8. Evaluation of cytotoxicity in primary leukemia cells (A) and normal lymphocytes (B) at 24 h (upper panel) and 48 h (lower panel). Leukemic lymphocytes were obtained from peripheral blood of patients with CLL (n = 4). Normal lymphocytes were obtained from peripheral blood of age-matched healthy donors (n = 3). Incubations were carried with or without (con) 10 μM compounds **1a**, **1c**, or **2** for 24 or 48 h, and the apoptosis induction was measured by annexin/PI binding assay. Each line represents one patient. The p value was obtained from Student's t tests (two tailed) performed using the GraphPad Prism5 software (GraphPad Software, Inc., San Diego, CA).

studied. The cross-linking efficiency of **1a**/H_2O_2 (50%) or **2**/H_2O_2 (55%) was close to that of **13** (52%) (Figure S9), which also supported our conclusion.

Determination of Specific Cross-Linking Sites and the Stability of Cross-Linked Products. The stability and reaction sites of the ICL products were examined to provide further insight into the reactivity of compounds **1a**–**e** and **2**. The reaction sites of DNA alkylation can be determined by investigating their heating stability under basic and/or neutral conditions. It was reported that the ICL induced by nitrogen mustards usually occurred at N-7 of dGs.[38] Piperidine is known to induce cleavage with N-7 alkylated purines upon heating.[39]

dx.doi.org/10.1021/jm401349g | J. Med. Chem. 2014, 57, 4498–4510

Thus, we examined the stability of DNA cross-linking products formed by these compounds in phosphate buffer (pH 7) or in 1.0 M piperidine (90 °C). The DNA ICLs were completely destroyed after heating for 30 min which led to obvious cleavage bands at dGs and dAs (Figure 6 and Figures S10–S13). These results are consistent with the observation that the reaction of nitrogen mustard mainly occurred at N7 of purines. However, in addition to major cleavage bands at the purine sites, we also observed some weak ones at pyrimidine nucleotides (e.g., 7–9, 16, 17, 19, 20, 59, 60, 65, 66, 68, and 72) as shown in Figure 6 and Figures S9–S11. Compared with other nitrogen mustards compounds,[22] such as mechlorethamine (Figure 6, lanes 7–9) and **13** (Figure 6, lanes 4–6), the cross-linking products induced by **1a–e** and **2** in the presence of H_2O_2 showed similar cleavage patterns as those induced by **13** (lanes 4–6) but were a little different from mechlorethamine. In a separate experiment, the ICL products and the drug-treated single stranded DNA were isolated from the reaction mixture and heated in neutral phosphate buffer or 1.0 M piperidine. Similar cleavage patterns were observed for ICL products and single stranded DNA (Figures S14 and S15). These data showed that apart from ICL formation, intrastrand cross-linking and/or monoalkylations were also possible.

Evaluation of the Cytotoxicities in Cell Lines. Since the activity of nitrogen mustards were effectively masked in **1a–e** and **2** but can be selectively triggered by H_2O_2 to induce efficient ICL formation, their cytotoxicity and selectivity were further evaluated in biological systems.[40] All of these agents showed significant growth inhibition of the cell lines tested. The growth percentages of most cell lines were less than 50% at a single dose of 10 μM. For comparison, **3** was also tested. However, no obvious toxicity was observed, which is consistent with the DNA cross-linking study. Furthermore, we compared the anticancer activity of the aromatic nitrogen mustards **1a** and **2** with that of **14** and **15** which released the simplest nitrogen mustard mechlorethamine.[26] Compounds **1a** and **2** showed a much higher growth-inhibitory effect on tumor cells than **14** and **15** (Figure 7). Although the precise mechanism underlying the higher toxicity of **1a** and **2** is not clearly understood yet, one of the possible reasons we considered is that **1a–e** and **2** are neutral molecules that are expected to diffuse across a cell membrane better than positively charged **14** and **15**.

Considering that different halogen groups (Br and Cl) in these compounds did not show much difference on the reactivity toward DNA and cytotoxicity toward cancer cell lines, compounds **1a**, **1c**, **1d**, and **2** were chosen as representative compounds to evaluate their GI_{50} (Table 1). All four compounds exhibited a high level of toxicity to the cell lines tested, such as leukemia, non-small-cell lung cancer, colon cancer, CNS cancer, melanoma, ovarian cancer, renal cancer, prostate cancer, and breast cancer. Although the GI_{50} toward these cell lines range from 0.23 to 31.4 μM, most of these compounds have a GI_{50} of less than 5 μM. In particular, they are more toxic toward leukemia, non-small-cell lung cancer, CNS cancer, renal cancer, and breast cancer than colon cancer, melanoma, and ovarian cancer. For example, a GI_{50} of about 1 μM was observed with cell lines SR (leukemia), NCI-H460 (non-small-cell lung cancer), and MDA-MB-468 (breast cancer). It was reported that leukemia, lung cancer, and breast cancer contain cells that proliferate under conditions of oxidative stress and have high intracellular concentrations of ROS.[41−44] It is very likely that these compounds can be more efficiently activated in these cells and therefore can lead to higher toxicity. In our initial DNA ICL study, compounds **1d** and **2** showed a little higher inducible DNA cross-linking ability than **1a**, but no obvious difference was observed with their cytotoxicity. Compound **2** with a boronic acid group had a little higher activity toward most cell lines than the other three with boronic esters (**1a**, **1c**, and **1d**), possibly due to its better water solubility (log P_{1a} = 2.8, log P_2 = 2.5; log P was determined in 1-octanol and PBS).

Apoptosis of CLL Cells or Normal Lymphocytes. Given that these compounds showed significant cytotoxicity in several cell lines, we investigated the selectivity of representative compounds (**1a**, **1c**, and **2**) in primary samples obtained from patients with CLL. CLL cells contain high levels of ROS and therefore should be effectively targeted by these agents. As expected, all three compounds (**1a**, **1c**, and **2**) induced significant amount of apoptosis in all samples tested. We observed a time (Figure 8A, 24 and 48 h, n = 4) and dose dependent apoptosis (Figure 9, 24 h, n = 3) in these samples.

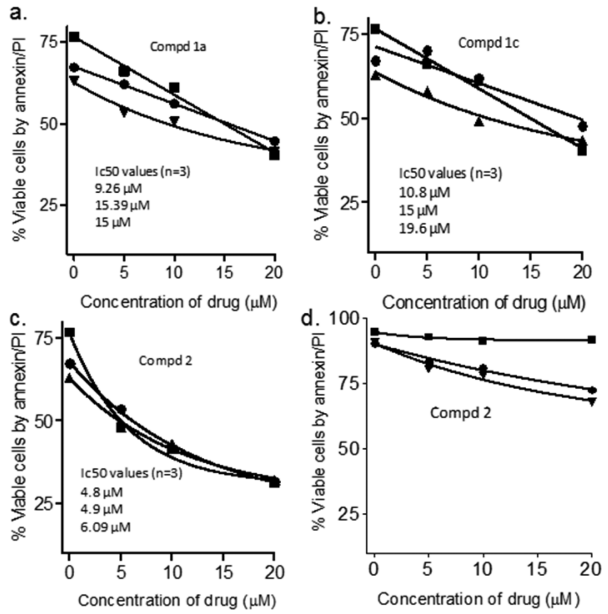

Figure 9. Dose-dependent apoptosis of CLL cells or normal lymphocytes with prodrugs **1a**, **1c**, **2**. Leukemic lymphocytes obtained from peripheral blood of patients with CLL (n = 3). Normal lymphocytes obtained from peripheral blood of age-matched healthy donors (n = 3). Incubations were carried with **1a**, **1c**, or **2** for 24 h, and the apoptosis induction was measured by annexin/PI binding assay: (A) CLL cells with **1a**; (B) CLL cells with **1c**; (C) CLL cells with **2**; (D) normal lymphocytes with **2** for 24 h.

Compared to compounds **1a** and **1c**, compound **2** demonstrated increased activities in CLL samples. The IC_{50} for the most potent compound (compound **2**) was between 5 and 6 μM.

To further assess the selectivity of these compounds toward cancer cells, we evaluated their toxicity toward normal lymphocytes isolated from peripheral blood of age-matched healthy donors (Figure 8B, 24 and 48 h, n = 3). Interestingly, **1a**, **1c**, and **2** resulted in comparatively less apoptosis, suggesting that the selective action toward cancer cells and the IC_{50} were not achieved in normal lymphocytes. Dose-dependent apoptosis of normal lymphocytes with prodrug **2** was achieved at 24 h. Compound **1a** at 24 h demonstrated % median for con-95, treated-93 (p = 0.226) and at 48 h the %

dx.doi.org/10.1021/jm401349g | J. Med. Chem. 2014, 57, 4498–4510

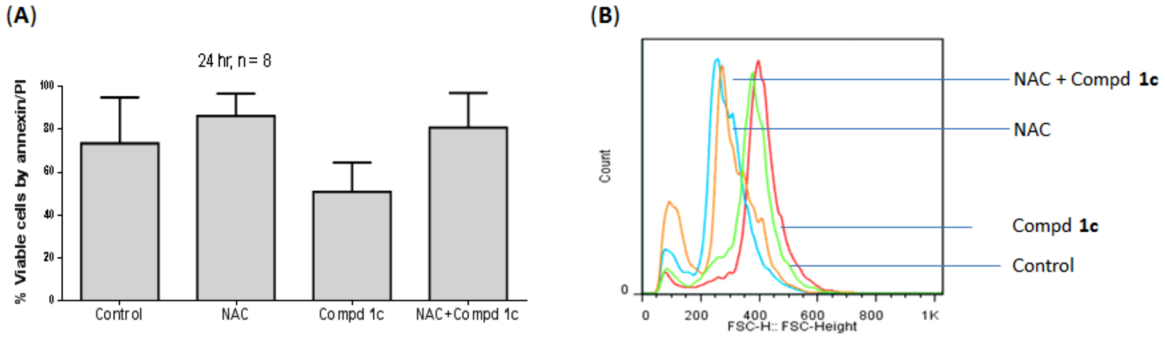

Figure 10. (A) Comparison of the apoptosis induced by ROS-activated prodrug **1c** in the presence or absence of *N*-acetyl cysteine (NAC). Primary CLL cells were incubated with compound **1c** in the absence or presence of NAC to block the production of ROS, and the cells were harvested at the end of 24 h. Apoptosis was measured by annexin/PI binding assay as described in the methods section. The error bars depict the mean SD for $n = 8$. (B) Comparison of the ROS level in CLL cells in the presence or absence of compound **1c** and/or NAC. Primary CLL cells were incubated with compound **1c** in the absence or presence of NAC (*N*-acetyl cysteine, 100 mM) to block the production of ROS. The cells were harvested at the end of 24 h, and the global ROS levels were measured by DCFDA staining as described in the materials and methods section. The histograms are provided for one representative patient sample ($n = 8$).

median for con-91, treated-83 ($p = 0.138$). Compound **1c** at 24 h demonstrated % median for con-95, treated-90 ($p = 0.111$) and at 48h % median for con-91, treated-81 ($p = 0.114$). Compound **2** at 24 h demonstrated % median for con-95, treated-92 ($p = 0.074$) and at 48 h % median for con-91, treated-83 ($p = 0.111$). CLL lymphocytes are known to have high ROS compared to normal lymphocytes.[45] This may be one of reasons why these compounds specifically kill leukemia cells while they spare normal lymphocytes.

Given that the H_2O_2-activated prodrugs are converted to active analogues in the presence of ROS, we postulated that blocking the ROS production by *N*-acetyl cysteine (NAC) should inhibit the cytotoxicity induced by these agents. To test our hypothesis, we incubated CLL lymphocytes with compound **1c** in the presence or absence of NAC and measured the end points such as cytotoxicity (by annexin/PI binding assay) and ROS production (by DCDFA assay). Our data showed that in the presence of NAC (100 mM) the apoptosis induced by **1c** (10 μM) was completely abrogated in eight patients tested (Figure 10A). Consistent with these results, incubation of **1c** in the presence of NAC further blocked the production of ROS (Figure 10B), suggesting that these agents function through ROS-dependent mechanisms. Data from one representative patient sample are shown in the right panel, but the experiment was done in six patient samples.

CONCLUSION

In summary, a series of ROS-activated aromatic nitrogen mustards with different leaving groups have been successfully synthesized. The boronate ester group sufficiently masks the activity of the aromatic nitrogen mustards which can be restored upon H_2O_2 treatment. The activation mechanism of these prodrugs by hydrogen peroxide was determined by NMR analysis. Among these agents with different leaving groups, compounds with methyl mesylate group showed more potent inducible DNA cross-linking ability than that with halogen groups, while there was no obvious difference in the reactivity of compounds with bromine or chlorine group. The stability study revealed that DNA cross-linking and/or alkylation induced by these agents mainly occurred with purine nucleotides. Consistent with the chemistry observation, in vitro cytotoxicity assay in respective cell lines demonstrated that these reagents exhibited effective killing of cancer cells with a concentration as low as or less than 1.0 μM. Higher toxicities were observed in cell lines, such as SR (leukemia), NCI-H460 (non-small-cell lung cancer), and MDA-MB-468 (breast cancer). In addition, these compounds showed selective toxicity toward primary leukemic lymphocytes from patients with chronic lymphocytic leukemia (40−80% apoptosis), while they were less toxic to normal lymphocytes from healthy donors (less than 25% cell death). The cellular study with or without an ROS quencher showed that these agents function through ROS-dependent mechanisms. Collectively, these data provide utility and selectivity of these agents which should inspire further and effective application in potential cancer chemotherapies.

EXPERIMENTAL SECTION

General Information. Unless otherwise specified, chemicals were purchased from Aldrich or Fisher Scientific and were used as received without further purification. T_4 polynucleotide kinase was purchased from New England Biolabs. Oligonucleotides were synthesized via standard automated DNA synthesis techniques using an Applied Biosystems model 394 instrument in a 1.0 μmole scale using commercial 1000 Å CPG-succinyl-nucleoside supports. Deprotection of the nucleobases and phosphate moieties and cleavage of the linker were carried out under mild deprotection conditions using a mixture of 40% aqueous $MeNH_2$ and 28% aqueous NH_3 (1:1) at room temperature for 2 h. [γ-^{32}P]ATP was purchased from Perkin-Elmer Life Sciences. Quantification of radiolabeled oligonucleotides was carried out using a Molecular Dynamics phosphorimager equipped with ImageQuant, version 5.2, software. ^{1}H NMR and ^{13}C NMR spectra were taken on either a Bruker DRX 300 or DRX 500 MHz spectrophotometer. Silicon reagents were used in $CDCl_3$ as internal standard. High resolution mass spectrometry was performed at the University of Kansas Mass Spectrometry Lab or University of California-Riverside Mass Spectrometry Lab. The purity was determined by RP-HPLC on a 4.6 mm × 250 mm RP-C18 column with 277 nm detection, which confirmed that all compounds had ≥95% purity.

Synthesis. 2,2′-(4-Bromophenylazanediyl)diethanol (6). A mixture of 4-bromoaniline (17.1 g, 0.1 mol), 2-chloroethanol (20 mL), $CaCO_3$ (20.0 g), and NaI (1.4 g) in 250 mL of water was heated to reflux overnight, then extracted with dichloromethane and washed with water. After evaporation of the solvent, the residue was purified by column chromatography (hexane/ethyl acetate = 1:2) to afford white solid **6** (18 g, 70%), mp 78−80 °C. ^{1}H NMR ($CDCl_3$, 300 MHz): δ 3.62 (t, $J = 4.8$ Hz, 4H), 3.88 (t, $J = 4.8$ Hz, 4H), 6.76 (d, $J = 8.4$ Hz, 2H), 7.38 (d, $J = 8.4$ Hz, 2H). ^{13}C NMR ($CDCl_3$, 75 MHz): δ

dx.doi.org/10.1021/jm401349g | J. Med. Chem. 2014, 57, 4498−4510

55.3, 60.5, 108.8, 114.2, 131.9, 146.8. HRMS-ES (m/z) $[M + H]^+$ calcd for $C_{10}H_{14}BrNO_2$, 260.0286; found, 260.0302.

2,2′-(4-(4,4,5,5-Tetramethyl-1,3,2-dioxaborolan-2-yl)-phenylazanediyl)diethanol (8). A mixture of **6** (3.8 g, 14.7 mmol), bis(pinacolato)diboron (7.4 g, 29.4 mmol), KOAc (4.3 g, 43.9 mol), and $PdCl_2$(dppf) (1.1 g, 1.5 mol) in dioxane (100 mL) was flushed with argon for 10 min and heated to reflux overnight under argon. After cooling to room temperature, the mixture was extracted with ethyl acetate and washed with brine. The organic layers were collected and dried over Na_2SO_4. After evaporation of the solvent under vacuum, the residue was purified by column chromatography (hexane/ethyl acetate = 1:2) to afford white foam **8** (2.52 g, 50%), mp 130−132 °C. ^{1}H NMR ($CDCl_3$, 300 MHz): δ 1.34 (s, 12H), 3.30 (br s, 2H), 3.65 (t, J = 4.5 Hz, 4H), 3.89 (t, J = 4.5 Hz, 4H), 4.08 (s, 2H), 6.71 (d, J = 8.4 Hz, 2H), 7.70 (d, J = 8.4 Hz, 2H). ^{13}C NMR ($CDCl_3$, 75 MHz): δ 24.8, 55.1, 60.6, 83.3, 111.4, 136.3, 150.1. HRMS-ES (m/z) $[M + H]^+$ calcd for $C_{16}H_{27}NO_4B$, 308.2033; found, 308.2013.

2,2′-(4-(4,4,5,5-Tetramethyl-1,3,2-dioxaborolan-2-yl)-phenylazanediyl)bis(ethane-2,1-diyl) Dimethanesulfonate (1f). To a solution of **8** (2.0 g, 5.83 mmol) and Et_3N (2.3 mL, 17.5 mmol) in dry CH_2Cl_2 (50 mL), MsCl (1.4 mL, 17.5 mmol) was added dropwise at 0 °C. After 30 min, the mixture was extracted with CH_2Cl_2 and washed with brine, water, dried over Na_2SO_4, and concentrated under vacuum. The residue was purified by column chromatography (hexane/ethyl acetate = 1:1) followed by recrystallization from EtOAc to afford white crystal solid **1f** (2.1 g, 80%), mp 85−86 °C. ^{1}H NMR ($CDCl_3$, 300 MHz): δ 1.33 (s, 12H), 2.96 (s, 6H), 3.81 (t, J = 5.7 Hz, 4H), 4.37 (t, J = 5.7 Hz, 4H), 6.71 (d, J = 9.0 Hz, 2H), 7.71 (d, J = 9.0 Hz, 2H). ^{13}C NMR ($CDCl_3$, 75 MHz): δ 24.9, 37.4, 50.4, 66.4, 83.4, 111.4, 136.7, 137.0, 148.5. HRMS-ES (m/z) $[M + Na]^+$ calcd for $C_{18}H_{30}NO_8S_2BNa$, 486.1404; found, 486.1387.

***N,N*-Bis(2-chloroethyl)-4-(4,4,5,5-tetramethyl-1,3,2-dioxaborolan-2-yl)aniline (1a).** A mixture of **1f** (926 mg, 2 mmol) and LiCl (84 mg, 2 mmol) in acetonitrile (5 mL) was stirred at 60 °C for 18 h. After removal of solvent, the residue was purified by column chromatography (hexane/ethyl acetate = 6:1) to afford white solid **1a** (233 mg, 34%), mp 79−80 °C. ^{1}H NMR ($CDCl_3$, 300 MHz): δ 1.35 (s, 12H), 3.66 (t, J = 6.9 Hz, 4H), 4.37 (t, J = 6.9 Hz, 4H), 6.68 (d, J = 8.7 Hz, 2H), 7.73 (d, J = 8.7 Hz, 2H). ^{13}C NMR ($CDCl_3$, 75 MHz): δ 24.8, 40.3, 53.3, 83.5, 111.0, 136.7, 148.3. HRMS-ES (m/z) $[M + H]^+$ calcd for $C_{16}H_{25}NO_2Cl_2B$, 344.1355; found, 344.1365.

Further elution with hexane/ethyl acetate 3:1 gave colorless oil **1d** (226 mg, 28%). ^{1}H NMR ($CDCl_3$, 300 MHz): δ 1.34 (s, 12H), 2.95 (s, 3H), 3.66 (t, J = 6.3 Hz, 2H), 3.75−3.83 (m, 4H), 4.34 (t, J = 5.7 Hz, 2H), 6.70 (d, J = 8.7 Hz, 2H), 7.72 (d, J = 8.7 Hz, 2H). ^{13}C NMR ($CDCl_3$, 75 MHz): δ 24.9, 37.5, 40.4, 50.3, 53.2, 66.4, 83.4, 111.2, 136.7, 148.5. HRMS-ES (m/z) $[M + H]^+$ calcd for $C_{17}H_{28}NO_5SBCl$, 404.1470; found,404.1497.

2-(2-Bromoethyl(4-(4,4,5,5-tetramethyl-1,3,2-dioxaborolan-2-yl)phenyl)amino)ethyl Methanesulfonate (1b). A mixture of **1f** (926 mg, 2 mmol) and LiBr (170 mg, 2 mmol) in acetonitrile (5 mL) was stirred at 60 °C for 20 h. After removal of solvent, the residue was purified by column chromatography (hexane/ethyl acetate = 6:1) to afford white solid **1b** (276 mg, 32%), mp 82−83 °C. ^{1}H NMR ($CDCl_3$, 300 MHz): δ 1.35 (s, 12H), 3.49 (t, J = 7.5 Hz, 4H), 3.83 (t, J = 7.5 Hz, 4H), 6.68 (d, J = 8.4 Hz, 2H), 7.74 (d, J = 8.4 Hz, 2H). ^{13}C NMR ($CDCl_3$, 75 MHz): δ 24.8, 28.1, 53.1, 83.4, 110.1, 136.8, 148.1. HRMS-EI (m/z) $[M + H]^+$ calcd for $C_{16}H_{25}BNO_2Br_2$, 432.0340; found, 432.0340.

Further elution with hexane/ethyl acetate 3:1 gave colorless oil **1e** (277 mg, 31%). ^{1}H NMR (DMSO-d_6, 300 MHz): δ 1.24 (s, 12H), 3.10 (s, 3H), 3.71−3.72 (m, 4H), 3.77 (t, J = 5.4 Hz, 2H), 4.30(t, J = 5.4 Hz, 2H), 6.75 (d, J = 8.4 Hz, 2H), 7.49 (d, J = 8.4 Hz, 2H). ^{13}C NMR ($CDCl_3$, 75 MHz): δ 24.9, 37.5, 40.4, 50.3, 53.2, 66.4, 83.4, 111.2, 136.7, 148.5. HRMS-ES (m/z) $[M - H + Na]^+$ calcd for $C_{17}H_{26}NO_5SBrBNa$, 469.0706; found, 469.0721.

***N*-(2-Bromoethyl)-*N*-(2-chloroethyl)-4-(4,4,5,5-tetramethyl-1,3,2-dioxaborolan-2-yl)aniline (1c).** A mixture of **1d** (806 mg, 2.0 mmol) and LiBr (170 mg, 2.0 mmol) in DMF (2 mL) was stirred at 60 °C for 4 h. The mixture was extracted with CH_2Cl_2, washed with brine, water, dried over Na_2SO_4, and concentrated under vacuum. The residue was purified by column chromatography (hexane/ethyl acetate = 10:1) to afford white foam **1c** (696 mg, 90%), mp 80−82 °C. ^{1}H NMR ($CDCl_3$, 500 MHz): δ 1.36 (s, 12H), 3.50 (t, J = 6.9 Hz, 2H), 3.66 (t, J = 6.9 Hz, 2H), 3.78 (t, J = 6.9 Hz, 2H), 3.84 (t, J = 6.9 Hz, 2H), 6.69 (d, J = 8.5 Hz, 2H), 7.75 (d, J = 8.5 Hz, 2H). ^{13}C NMR ($CDCl_3$, 75 MHz): δ 24.9, 28.2, 40.4, 53.0, 53.3, 83.4, 110.9, 136.6, 148.2. HRMS-EI (m/z) $[M]^+$ calcd for $C_{16}H_{24}BNO_2ClBr$: 368.0807; found, 368.0803.

4-Bromo-*N,N*-bis(2-chloroethyl)aniline (9). A solution of MsCl (0.9 mL, 11.5 mmol) in DCM (5 mL) was added dropwise to a mixture of **6** (1.0 g, 3.85 mmol) and Et_3N (1.5 mL, 11.5 mmol) in dry CH_2Cl_2 (20 mL) at 0 °C. After 30 min, the mixture was extracted with CH_2Cl_2 twice and the combined organic phase was washed with brine, water, dried over Na_2SO_4, and then concentrated under vacuum. The residue was used in the next step without further purification. The residue was dissolved in DMF (8 mL), and LiCl (966 mg, 23.0 mmol) was added. After being stirred at 70 °C for 5 h, the mixture was extracted with CH_2Cl_2 and washed with brine, water, dried over Na_2SO_4, and concentrated under vacuum. The residue was purified by column chromatography (hexane/ethyl acetate = 10:1) to afford white foam **9** (1.1 g, 91%), mp 65−67 °C. ^{1}H NMR ($CDCl_3$, 300 MHz): δ 3.62−3.66 (m, 4H), 3.71−3.76 (m, 4H), 6.60 (d, J = 9.0 Hz, 2H), 7.35 (d, J = 9.0 Hz, 2H). ^{13}C NMR ($CDCl_3$, 75 MHz): δ 40.4, 53.5, 109.7, 113.8, 132.5, 145.2. HRMS-EI (m/z) $[M]^+$ calcd for $C_{10}H_{12}NCl_2Br$, 294.9525; found, 294.9526.

4-(Bis(2-chloroethyl)amino)phenylboronic Acid (2). A solution of **9** (1.8 g, 6 mmol) in dry THF (60 mL) was cooled to −78 °C under Ar. ^{n}BuLi (8.6 mL, 2.6 M in hexane) was added slowly at the same temperature within 10 min. After 30 min, $B(O^iPr)_3$ (2.9 g, 15 mmol) was added. The mixture was allowed to warm to room temperature and stirred overnight, then quenched by NH_4Cl solution at 0 °C. The mixture was extracted with CH_2Cl_2 and washed with water, dried over Na_2SO_4, and concentrated under vacuum. The residue was purified by column chromatography (hexane/ethyl acetate = 1:1) to afford white solid **2** (1.06 g, 68%), mp 203−205 °C. ^{1}H NMR (DMSO-d_6 + D_2O, 300 MHz): δ 3.69−3.71 (m, 8H), 6.67 (d, J = 8.7 Hz, 2H), 7.60 (d, J = 8.7 Hz, 2H). ^{13}C NMR (DMSO-d_6 + D_2O, 75 MHz): δ 41.7, 52.3, 111.4, 136.2, 148.6. HRMS-EI (m/z) $[M + H]^+$ calcd for $C_{10}H_{15}BNO_2Cl_2$, 262.0567; found, 262.0573.

4-(4,4,5,5-Tetramethyl-1,3,2-dioxaborolan-2-yl)benzylbis(2-chloroethyl)carbamate (3). To a suspension of bis(2-chloroethyl)-amine hydrochloride (1.24 g, 7.0 mmol) in DMF (50 mL), DMAP (1.02 g, 8.4 mmol) was added. The mixture was stirred at room temperature for 30 min, and then **11** (415 mg, 1.4 mmol) was added. The resulting mixture was further stirred at 60 °C overnight and extracted with CH_2Cl_2. The organic layer was washed with water, dried over Na_2SO_4, and concentrated in vacuo. The residue was purified by column chromatography (hexane/ethyl acetate = 5:1) to afford colorless oil **3** (170 mg, 30%). ^{1}H NMR ($CDCl_3$, 500 MHz): δ 1.29 (s, 12H), 3.62 (t, J = 6.0 Hz, 4H), 3.72−3.74 (m, 4H), 5.13 (s, 2H), 7.37 (d, J = 7.5 Hz, 2H), 7.68 (d, J = 7.5 Hz, 2H). ^{13}C NMR ($CDCl_3$, 125 MHz): δ 25.1, 42.0, 42.5, 49.1, 49.5, 66.9, 84.1, 127.4, 135.0, 140.4, 155.6. HRMS-ES (m/z) $[M + Na]^+$ calcd for $C_{18}H_{26}BNO_4NaCl_2$, 424.1224; found, 424.1240.

Detection of DNA Cross-Linking. ICL formation and cross-linking yields were analyzed via denaturing polyacrylamide gel electrophoresis (PAGE) with phosphorimager analysis. The DNA−DNA cross-linking abilities of these compounds were investigated by reacting with a ^{32}P-labeled 49-mer oligonucleotide **12** (Figure 1) and then subjected to 20% denaturing PAGE analysis. The ^{32}P-labeled oligonucleotide **12a** (1.0 μM) was annealed with 1.5 equiv of the complementary strand **12b** by heating to 65 °C for 3 min in a buffer of 10 mM potassium phosphate (pH 7) and 100 mM NaCl, followed by slow-cooling to room temperature overnight. The ^{32}P-labeled duplex DNA (2 μL, 1.0 μM) was mixed with 1.0 M NaCl (2 μL), 100 mM potassium phosphate (2 μL, pH 8), 10 μM to 50 mM H_2O_2 (2 μL), and 10 μM to 50 mM compounds **1a−f** and **2** (resulting in a concentration range of 1 μM to 5 mM), and appropriate amount of autoclaved distilled water was added to give a final volume of 20 μL.

dx.doi.org/10.1021/jm401349g | J. Med. Chem. 2014, 57, 4498−4510

The reaction mixture was incubated at room temperature for 16 h and then quenched by an equal volume of 90% formamide loading buffer. Finally it was subjected to 20% denaturing polyacrylamide gel analysis.

Cell Lines. The in vitro cancer cell screen was performed at the National Cancer Institute (NCI Developmental Therapeutics Program). The procedure details can be found in NCI Web site: http://dtp.nci.nih.gov/branches/btb/ivclsp.html (Methodology of the in Vitro Cancer Screen). The human tumor cell lines were grown in RPMI 1640 medium containing 5% fetal bovine serum and 2 mM L-glutamine. Cells are inoculated into 96-well microtiter plates in 100 μL at plating densities ranging from 5000 to 40 000 cells/well depending on the doubling time of individual cell lines.

CLL Cells and Normal Lymphocytes. Leukemic lymphocytes were isolated from fresh peripheral blood sample obtained from patients with CLL. Separate laboratory protocols were used to obtain blood samples from patients with CLL and healthy donors. All individuals signed written informed consent forms in accordance with the Declaration of Helsinki and with the laboratory protocols approved by the institutional review board at the University of Texas MD Anderson Cancer Center.

(A) Isolation of CLL and Normal Lymphocytes. Whole blood was collected in heparinized tubes and diluted 1:3 with cold PBS (0.135 M NaCl, 2.7 mM KCl, 1.5 mM KH_2PO_4, 8 mM Na_2HPO_4 [pH 7.4]) and layered onto Ficoll-Hypaque (specific gravity, 1.086; Life Technologies, Grand Island, NY). The blood was then centrifuged at 433*g* for 20 min, and mononuclear cells were removed from the interphase. Cells were washed twice with cold PBS and resuspended in 10 mL of RPMI 1640, supplemented with 10% autologous plasma. A Coulter channelyzer (Coulter Electronics, Hialeah, FL) was used to determine cell number and the mean cell volume. The CLL or normal lymphocytes were suspended in medium at a concentration of 1×10^7 cells/mL, and fresh cells were used for all experiments.

(B) Measurement of Apoptosis. Cell death is evaluated by flow cytometry analysis with the use of annexin V−PI double staining. CLL or normal lymphocytes in suspension are incubated with 10 μM compounds, and the cell death was measured by annexin V binding assay. Time matched control samples with no drug are also maintained side by side. At the end of incubation time, cells are washed with PBS and resuspended in 200 μL of 1× annexin binding buffer (BD Biosciences) at a concentration of 1×10^6 cells/mL. Annexin V−FITC (5 μL) is added, and the cells are incubated in the dark for 15 min at room temperature. A total of 10 μL of PI (50 μg/mL) is added to the labeled cells and analyzed immediately with a FACSCALIBUR cytometer (Becton Dickinson). Data from at least 10 000 events per sample are recorded and processed using Cell Quest software (Becton Dickinson).

■ ASSOCIATED CONTENT

Supporting Information

Experimental procedures for reactions and analysis, characterization of **1**−**13**, autoradiograms of Fe·EDTA, and piperidine treatment of cross-linked products and reacted single-stranded DNA. This material is available free of charge via the Internet at http://pubs.acs.org.

■ AUTHOR INFORMATION

Corresponding Author

*E-mail: pengx@uwm.edu. Phone: 414-229-5221.

Notes

The authors declare no competing financial interest.

■ ACKNOWLEDGMENTS

We are grateful for the financial support for this research from the National Cancer Institute (Grant 1R15CA152914-01) and Chronic Lymphocytic Leukemia Research Consortium (Grant 2 PO1 CA 81534), Great Milwaukee Foundation (Shaw Scientist Award), and UWM startup funds.

■ ABBREVIATIONS

ROS, reactive oxygen species; CLL, chronic lymphocytic leukemia cell; ICL, interstrand cross-link; MsCl, methanesulfonyl chloride; TBHP, *tert*-butyl hydroperoxide; SR, leukemia cell; NCI-H460, non-small-cell lung cancer cells; MDA-MB-468, breast cancer cells; NAC, *N*-acetyl cysteine

■ REFERENCES

(1) Szatrowski, T. P.; Nathan, C. F. Production of large amounts of hydrogen peroxide by human tumor cells. *Cancer Res.* **1991**, *51*, 794−798.

(2) Toyokuni, S.; Okamoto, K.; Yodoi, J.; Hiai, H. Persistent oxidative stress in cancer. *FEBS Lett.* **1995**, *358*, 1−3.

(3) Schumacker, P. T. Reactive oxygen species in cancer cells: live by the sword, die by the sword. *Cancer Cell* **2006**, *10*, 175−176.

(4) Lim, S. D.; Sun, C.; Lambeth, J. D.; Marshall, F.; Amin, M.; Chung, L.; Petros, J. A.; Arnold, R. S. Increased Nox1 and hydrogen peroxide in prostate cancer. *Prostate* **2005**, *62*, 200−207.

(5) Zieba, M.; Suwalski, M.; Kwiatkowska, S.; Piasecka, G.; Grzelewska-Rzymowska, I.; Stolarek, R.; Nowak, D. Comparison of hydrogen peroxide generation and the content of lipid peroxidation products in lung cancer tissue and pulmonary parenchyma. *Respir. Med.* **2000**, *94*, 800−805.

(6) Hileman, E. O.; Liu, J.; Albitar, M.; Keating, M. J.; Huang, P. Intrinsic oxidative stress in cancer cells: a biochemical basis for therapeutic selectivity. *Cancer Chemother. Pharmacol.* **2004**, *53*, 209−219.

(7) Trachootham, D.; Alexandre, J.; Huang, P. Targeting cancer cells by ROS-mediated mechanisms: a radical therapeutic approach? *Nat. Rev.* **2009**, *8*, 579−591.

(8) Pelicano, H.; Lu, W.; Zhou, Y.; Zhang, W.; Chen, Z.; Hu, Y.; Huang, P. Mitochondrial dysfunction and reactive oxygen species imbalance promote breast cancer cell motility through a CXCL14-mediated mechanism. *Cancer Res.* **2009**, *69*, 2375−2383.

(9) Lopez-Lazaro, M. Dual role of hydrogen peroxide in cancer: possible relevance to cancer chemoprevention and therapy. *Cancer Lett.* **2007**, *252*, 1−8.

(10) Trachootham, D.; Zhou, Y.; Zhang, H.; Demizu, Y.; Chen, Z.; Pelicano, H.; Chiao, P. J.; Achanta, G.; Arlinghaus, R. B.; Liu, J.; Huang, P. Selective killing of oncogenically transformed cells through a ROS-mediated mechanism by beta-phenylethyl isothiocyanate. *Cancer Cell* **2006**, *10*, 241−252.

(11) Peng, H.; Li, F.; Elizabeth, A. O.; Michael, J. K.; William, P. Superoxide dismutase as a target for the selective killing of cancer cells. *Nature* **2000**, *407*, 390−395.

(12) Pelicano, H.; Feng, L.; Zhou, Y.; Carew, J. S.; Hileman, W. P.; Keating, M. J.; Huang, P. Inhibition of mitochondrial respiration: a novel strategy to enhance drug-induced apoptosis in human cells by a reactive oxygen species-mediated mechanism. *J. Biol. Chem.* **2003**, *278*, 37832−37839.

(13) Raj, L.; Ide, T.; Gurkar, A. U.; Foley, M.; Schenone, M.; Li, X.; Tolliday, N. J.; Golub, T. R.; Carr, S. A.; Shamji, A. F.; Stern, A. M.; Mandinova, A.; Schreiber, S. L.; Lee, S. W. Selective killing of cancer cells by a small molecule targeting the stress response to ROS. *Nature* **2011**, *475*, 231−234.

(14) Adamsa, D.; Daia, M.; Pellegrinoa, G.; Wagnera, B. K.; Sterna, A. M.; Shamjia, A. F.; Schreibera, S. L. Synthesis, cellular evaluation, and mechanism of action of piperlongumine analogs. *Proc. Natl. Acad. Sci. U.S.A.* **2012**, *109*, 15115−15120.

(15) Chowdhury, G.; Junnotula, V.; Daniels, J. S.; Greenberg, M. M.; Gates, K. S. DNA strand damage product analysis provides evidence that the tumor cell-specific cytotoxintirapazamine produces hydroxyl radical and acts as a surrogate for O_2. *J. Am. Chem. Soc.* **2007**, *129*, 12870−12877.

(16) Junnotula, R.; Rajapakse, A.; Arbillaga, L.; Lopez de Cerain, A.; Solano, B.; Villar, R.; Monge, A.; Gates, K. S. DNA strand cleaving properties and hypoxia-selective cytotoxicity of 7-chloro-2-thienylcar-

bonyl-3-trifluoromethylquinoxaline 1,4-dioxide. *Bioorg. Med. Chem.* **2010**, *18*, 3125−3132.
(17) Junnotula, V.; Sarkar, U.; Sinha, S.; Gates, K. S. Initiation of DNA strand cleavage by 1,2,4-benzotriazine 1,4-dioxide antitumor agents: mechanistic insight from studies of 3-methyl-1,2,4-benzotriazine 1,4-dioxide. *J. Am. Chem. Soc.* **2009**, *130*, 1015−1024.
(18) Noll, D. M.; Mason, T. M.; Miller, P. S. Formation and repair of interstrand cross-links in DNA. *Chem. Rev.* **2006**, *106*, 277−301.
(19) Antonio, M. D.; Doria, F.; Mella, M.; Merli, D.; Profumo, A.; Freccero, M. Novel naphthalene diimides as activatable precursors of bisalkylating agents, by reduction and base catalysis. *J. Org. Chem.* **2007**, *72*, 8354−8360.
(20) Verga, D.; Nadai, M.; Doria, F.; Percivalle, C.; Antonio, M. D.; Palumbo, M.; Richter, S. N.; Freccero, M. Photogeneration and reactivity of naphthoquinonemethides as purine selective DNA alkylating agents. *J. Am. Chem. Soc.* **2010**, *132*, 14625−14637.
(21) Percivalle, C.; Rosa, A. L.; Verga, D.; Doria, F.; Mella, M.; Palumbo, M.; Antonio, M. D.; Freccero, M. Quinone methide generation via photoinduced electron transfer. *J. Org. Chem.* **2011**, *76*, 3096−3106.
(22) Hong, I. S.; Greenberg, M. M. DNA interstrand cross-link formation initiated by reaction between singlet oxygen and a modified nucleotide. *J. Am. Chem. Soc.* **2005**, *127*, 10510−10511.
(23) Peng, X.; Hong, I. S.; Li, H.; Seidman, M. M.; Greenberg, M. M. Interstrand cross-link formation in duplex and triplex DNA by modified pyrimidines. *J. Am. Chem. Soc.* **2008**, *130*, 10299−10306.
(24) Veldhuyzen, W. F.; Pande, P.; Rokita, S. E. A transient product of DNA alkylation can be stabilized by binding localization. *J. Am. Chem. Soc.* **2003**, *125*, 14005−14013.
(25) Richter, S. N.; Maggi, S.; Mels, S. C.; Palumbo, M.; Freccero, M. Binolquinonemethides as bisalkylating and DNA cross-linking agents. *J. Am. Chem. Soc.* **2004**, *126*, 13973−13979.
(26) Kuang, Y.; Balakrishnan, K.; Gandhi, V.; Peng, X. Hydrogen peroxide inducible DNA cross-linking agents: targeted anticancer prodrugs. *J. Am. Chem. Soc.* **2011**, *133*, 19278−19281.
(27) Cao, S.; Wang, Y.; Peng, X. ROS-Inducible DNA cross-linking agent as a new anticancer prodrug building block. *Chem.—Eur. J.* **2012**, *18*, 3850−3854.
(28) (a) Pelicano, H.; Carney, D.; Huang, P. ROS stress in cancer cells and therapeutic implications. *Drug Resist. Updates* **2004**, *7*, 97−110. (b) Burdon, R. H. Superoxide and hydrogen peroxide in relation to mammalian cell proliferation. *Free Radical Biol. Med.* **1995**, *18*, 775−794. (c) Lopez-Lazaro, M. HIF-1: hypoxia-inducible factor or dysoxia-inducible factor? *FASEB J.* **2006**, *20*, 828−832.
(29) Hall, D. G. Structure, Properties, and Preparation of Boronic Acid Derivatives. Overview of Their Reactions and Applications. In *Boronic Acids: Preparation and Applications in Organic Synthesis and Medicine*; Hall, D. G., Ed.; Wiley-VCH Verlag GmbH & Co. KGaA: Weinheim, Germany, 2006.
(30) Srikun, D.; Miller, E. W.; Domaille, D. W.; Chang, C. J. An ICT-based approach to ratiometric fluorescence imaging of hydrogen peroxide produced in living cells. *J. Am. Chem. Soc.* **2008**, *130*, 4596−4597.
(31) Dickinson, B. C.; Huynh, C.; Chang, C. J. A palette of fluorescent probes with varying emission colors for imaging hydrogen peroxide signaling in living cells. *J. Am. Chem. Soc.* **2010**, *132*, 5906−5915.
(32) Major Jourden, J. L.; Cohen, S. M. Hydrogen peroxide activated matrix metalloproteinase inhibitors: a prodrug approach. *Angew. Chem., Int. Ed.* **2010**, *49*, 6795−6797.
(33) Govan, J. M.; McIver, A. L.; Riggsbee, C.; Deiter, A. Hydrogen peroxide induced activation of gene expression in mammalian cells using boronate estrone derivatives. *Angew. Chem., Int. Ed.* **2012**, *51*, 9066−9070.
(34) Lewis, G. G.; DiTucci, M. J.; Phillips, S. T. Quantifying analytes in paper-based microfluidic devices without using external electronic readers. *Angew. Chem., Int. Ed.* **2012**, *51*, 12707−12710.
(35) Peng, X.; Gandhi, V. ROS-activated anticancer prodrugs: a new strategy for tumor-specific damage. *Ther. Delivery* **2012**, *7*, 823−833.
(36) Hagen, H.; Marzenell, P.; Jentzsch, E.; Wenz, F.; Veldwijk, M. R.; Mokhir, A. Aminoferrocene-based prodrugs activated by reactive oxygen species. *J. Med. Chem.* **2012**, *55*, 924−934.
(37) Marzenell, P.; Hagen, H.; Sellner, L.; Zenz, T.; Grinyte, R.; Pavlov, V.; Daum, S.; Mokhir, A. Aminoferrocene-based prodrugs and their effects on human normal and cancer cells as well as bacterial cells. *J. Med. Chem.* **2013**, *56*, 6935−6944.
(38) (a) Hemmimki, K.; Kallama, S. Reactions of Nitrogen Mustards with DNA. In *Carcinogenicity of Alkylating Cytostatic Drugs*; Schmahl, D., Kaldor, J. M.. Eds.; IARC Publication No. 78; International Agency for Research on Cancer: Lyon, France, 1986; pp 55−70. (b) Pieper, O. P.; Erickson, L. C. DNA adenine adducts induced by nitrogen mustards and their role in transcription termination in vitro. *Carcinogenesis* **1990**, *11*, 1739−1746. (c) Brookes, P.; Lawley, P. D. The reaction of mono- and di-functional alkylating agents with nucleic acids. *Biochem. J.* **1961**, *80*, 496−503.
(39) (a) Maxam, A. M.; Gilbert, W. A new method for sequencing DNA. *Proc. Natl. Acad. Sci. U.S.A.* **1977**, *74*, 560−564. (b) Haraguchi, K.; Delaney, M. O.; Wiederholt, C. J.; Sambandam, A.; Hantosi, Z.; Greenberg, M. M. Synthesis and characterization of oligodeoxy nucleotides containing formamidopyrimidine lesions and nonhydrolyzable analogues. *J. Am. Chem. Soc.* **2002**, *124*, 3263−3269. (c) Peng, X.; Hong, I. S.; Li, H.; Seidman, M. M.; Greenberg, M. M. Interstrand cross-link formation in duplex and triplex DNA by modified pyrimidines. *J. Am. Chem. Soc.* **2008**, *130*, 10299−10306.
(40) Data were obtained from Developmental Therapeutics Program at the National Cancer Institute (NCI-60 DTP Human Tumor Cell Line Screen): http://dtp.nci.nih.gov/index.html.
(41) Brown, N. S.; Bicknell, R. Hypoxia and oxidative stress in breast cancer: oxidative stress: its effects on the growth, metastatic potential and response to therapy of breast cancer. *Breast Cancer Res.* **2001**, *3*, 323−327.
(42) Veni, G. K.; Rao, D. B.; Kumar, M.; Usha, B.; Krishma, M.; Rao, T. R. Clinical evaluation of oxidative stress in women with breast cancer. *Recent Res. Sci. Technol.* **2011**, *3*, 55−58.
(43) Tas, F.; Hansel, H.; Belce, A.; Ilvan, S.; Argon, A.; Camlica, H.; Topuz, E. Oxidative stress in breast cancer. *Med. Oncol.* **2005**, *22*, 11−15.
(44) Zieba, M.; Suwalski, M.; Kwiatkowska, S.; Piasecka, G.; Grzelewska-Rzymowska, I.; Stolarek, R.; Nowak, D. Comparison of hydrogen peroxide generation and the content of lipid peroxidation products in lung cancer tissue and pulmonary parenchyma. *Respir. Med.* **2000**, *94*, 800−805.
(45) Trachootham, D.; Zhang, H.; Zhang, W.; Feng, L.; Du, M.; Zhou, Y.; Chen, Z.; Pelicano, H.; Plunkett, W.; Wierda, W. G.; Keating, M. J.; Huang, P. Effective elimination of fludarabine-resistant CLL cells by PEITC through a redox-mediated mechanism. *Blood* **2008**, *112*, 1912−1922.